Trapping and Sorting Micro-Nano Particles in a Dynamic Optical Sieve

Jian Chen, Dongmei Liu, Jian Qiu, Li Peng, Kaiqing Luo, and Peng Han

***Abstract*—We propose a novel strategy for optical trapping and sorting of micro-nano particles that does not involve the flow of the immersion medium. The method employs the size- and velocity-dependent response of suspended polystyrene particles to the optical sieve of a dynamic fringelike pattern generated by a spatial light modulator. We not only experimentally demonstrate the trapping and transport of polystyrene particles with 2 μm diameter, but also study the sorting of a polydisperse suspension of polystyrene beads with diameters of 0.8 and 2 μm. The results provide new insights into particle manipulation and separation, and reveal that there is still scope for sorting smaller particles based on dynamic optical sieve.**

***Index Terms*—Dynamic optical sieve, optical micromanipulation, spatial light modulator, fringe-like optical field.**

I. Introduction

PRECISE manipulation of micro- and nano-objects has been attracting increasing attention in recent years, particularly because of the increasing number of applications, such as nanofabrication [1], [2], disease diagnostics [3], [4], drug delivery [5], [6], and bioanalysis [7], [8], [9]. However, current micromanipulation methods are generally limited by their efficiency and throughput. For example, the single-beam optical trap, which consists of a single Gaussian beam focused by a high-numerical-aperture objective, can only trap one or a few particles in aqueous solution at a time. Many efforts have been made to overcome these constraints. Several approaches have been developed to produce complex patterns [10], assembled arrays [11], modulated structures [12], [13], self-driven micro-bots [14], [15], and artificial cilia [16], [17], [18]. These approaches use many diverse technologies including hydrodynamic, magnetic, optical, acoustic, and electrical fields. In the field of optics, the micromanipulation mainly relies on the momentum carried by laser beam, which interacts with matter and yields a force to influence the motion of small objects. The first attempt to manipulate microscopic particles can be traced back to the study conducted by Ashkin [19] in 1970, in which the Author proved that micrometer-sized dielectric particles can be trapped by two counter-propagating beams. Since then, investigations of optical micromanipulation and its applications in biomedicine, chemistry, and physics have become an active research area.

Recently, an optical potential energy landscape was proposed to trap multiple particles at a time. However, the optical potential fields are mainly generated through optical diffractive elements [20], [21] that may require high-end process technology. Furthermore, one-dimensional lattices or interference patterns have been proposed to sort particles in the absence of microfluidic flow [22], [23], [24]. But to the best of our knowledge, few experiments using dynamically optical landscapes have been reported [25], [26]. In most of these researches, the performance of the generated optical landscape, such as its pattern, size, and moving velocity, are fixed in the devices. The few tunable methods require certain complicated mechanisms, such as the interference of multi-beams [27], [28], [29].

II. Basic Principle

In this study, we demonstrate an optical micromanipulation system, i.e., dynamic optical sieve, to achieve flexibility and high throughput by exploiting the sizes and velocities of the optical landscapes generated from a spatial light modulator (SLM). Our system does not require microfluidic flow, but implements fringe patterns moving with a tunable size and velocity. The basic physics behind this experiment is schematically illustrated in Fig. 1(a). Shaped by the Gaussian beam, the intensity profile of fringe optical field follows the function of $I(x,y) = \frac{2P}{\pi\omega_0^2}\ cos^2\frac{\pi x}{\Lambda} exp[-2(x^2+y^2)^2/\omega_0^2]$, where Λ is the spatial size of the fringe, P is the input power of the laser, and ω_0 is the beam waist of the laser. The bright fringe produces localized intensity gradient forces that can draw the particles toward the focus in this optical field. These forces stably capture particles of a given size, such as the particle A in Fig. 1(a), which is bound to the center of bright fringes. Correspondingly, the particle B cannot be trapped by the bright stripes and would continue to present Brownian motion in the solution. If the fringe field is given a velocity, the trapped particle A will move along with the bright stripes. Therefore, the moving stripe optical field can be used to realize the separation of particles A and B. This phenomenon is similar to a dynamic optical sieve, where the

Manuscript received October 30, 2021; revised December 28, 2021; accepted February 1, 2022. Date of publication February 8, 2022; date of current version February 17, 2022. This work was supported in part by the National Natural Science Foundation of China under Grant 61975058, in part by the Natural Science Foundation of Guangdong Province under Grant 2019A1515011401, in part by the Science and Technology Program of Guangzhou under Grant 2019050001, and in part by the the Science and Technological Plan of Guangdong Province, China under Grant 2019B090905005. *(Corresponding authors: Dongmei Liu; Peng Han.)*

The authors are with the Guangdong Provincial Engineering Research Center for Optoelectronic Instrument, School of Physics and Telecommunication Engineering, South China Normal University, Guangzhou 510006, China, and also with SCNU Qingyuan Institute of Science and Technology Innovation Company Ltd., Qingyuan 511517, China (e-mail: chenjian@m.scnu.edu.cn; dmliu@scnu.edu.cn; qiuj@scnu.edu.cn; pengli@m.scnu.edu.cn; kqluo@scnu.edu.cn; hanp@scnu.edu.cn).

Digital Object Identifier 10.1109/JPHOT.2022.3149282

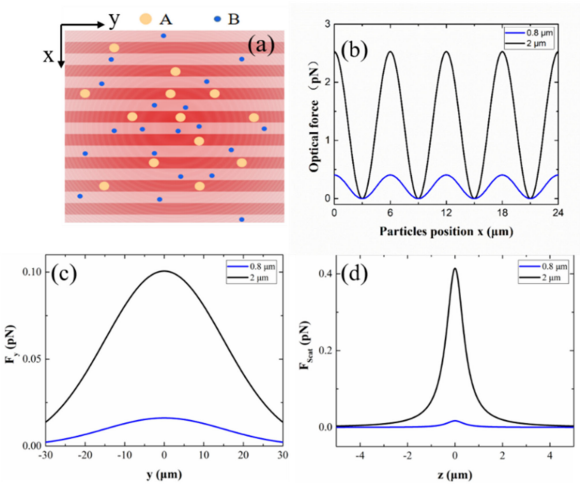

Fig. 1. Manipulation principle of dynamic optical sieve (a), the red stripes, white stripes and yellow lines represent the bright stripes, dark stripes and Gaussian beam profile, respectively. The optical forces of two polystyrene particles with diameters of 0.8 and 2 μm in x direction (b), y direction (c), and z direction (z), respectively. The laser power is 40 mW and the spatial size of fringe is 3 μm.

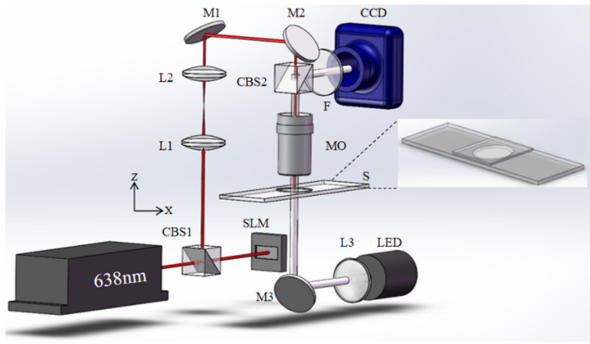

Fig. 2. Schematic of experimental setup for optical trapping and sorting of particles in dynamic fringes optical field: Laser, semiconductor laser with a wavelength of 638 nm; CBS, cube beam splitter; SLM, spatial light modulator, L1, L2, L3, lenses; M1, M2, M3, mirrors; MO, micro-objective; S, sample cell; CCD, charge coupled device; LED, light emitting diode; F, filter.

particles of a given size can be continuously swept to one place, but the particles of other sizes will escape from it. Moreover, we can further adjust the separating speed of particles by changing the moving speed of the optical sieve.

Besides, we theoretically calculated the optical forces of particles of different sizes in our fringe optical field. According to the generalized Lorenz-Mie theory [30], [31] in the interaction of light and matter, it is assumed that the polystyrene sphere is located on the point (x_0, y_0) of mid-plane $(z = 0)$ of the sample cell, the localized gradient force [32] generated by fringe optical field is given by (1), shown at bottom of this page.

Where n_m is the refractive index of the polystyrene particle, r is the radius of the particles, and c is the speed of light in vacuum. R and T are the reflectance and transmittance coefficients. θ_i and φ are the polar and azimuthal angles in spherical coordinates, respectively, while the transmitted angle is denoted by θ_o.

Except for gradient force F_z, the trapped particles also experienced the scattering force in z direction, which can be written as

$$F_{scat} = \frac{8}{3}\pi(kr)^4 r^2 \left(\frac{m^2-1}{m^2+2}\right)^2 \frac{n_m}{c} \times I(x,y) \qquad (2)$$

Where $m = \mathrm{n_m/n_1}$ is the effective index, $\mathrm{n_1}$ is the refractive of the aqueous solution, $\mathrm{k} = \frac{2\pi}{\lambda}$ is the wave vector, and λ is the wavelength of input laser. We chose polystyrene spheres with diameters of 0.8 and 2 μm in the theoretical calculation. The incident laser power was 40 mW, the beam waist radius was 40 μm, and the size of fringes was 3 μm. The refractive of aqueous solution is $\mathrm{n_1} = 1.33$. As is shown in Fig. 1(b), the gradient forces in x direction change periodically with the particle position (black and blue lines). For 2-μm and 0.8-μm polystyrene particles, the calculations yield the optical force of 2.5 pN and 0.4 pN, respectively. Therefore, the bright fringes can easily trap the 2-μm particles, but the restraint effect on 0.8-μm particles is weak.

As mentioned above, the trapped particles also experienced the optical force from y and z directions. According to (1) and (2), we calculated the optical forces in y and z directions. In comparison with the scattering force F_{scat}, the gradient force F_z can be negligible for the trapped particles. Fig. 1(c) and 1(d) show the gradient force F_y and scattering force F_{scat}, respectively. From Fig. 1(b) to Fig. 1(d), we notice that that the intensity gradient force in x direction (2.5 pN for 2-μm particle) is much larger than those in other two directions (0.1 pN in y direction and 0.4 pN in z direction), which is a strong evidence of trapping ability of optical sieve. As we expected, when the bright fringes move at a given velocity, which will push 2-μm particles get together, while the movement of 0.8-μm particles is almost unaffected. Compared with the 2-μm particles, the Brownian motion of 0.8-μm particles is more intense, which requires greater force to be trapped. We thus expect the dynamic fringelike field to drive larger particles to one place and realize the separation of 2-μm and 0.8-μm particles at the laser power of 40 mW, which is also consistent with our experimental results (see Fig. 5).

III. Experimental Setup

Different from our previous study on diffusion of Brownian particles [33], the particle manipulating setup is schematically shown in Fig. 2. A phase-only spatial light modulator (SLM) (HOLOEYE, GAEA-VIS-069) to imprint computer-generated holograms on a laser beam (semiconductor laser, 0638 L-11A-NI-NT-NF) at a vacuum wavelength of 638 nm. The modulated beam is retransmitted to an objective lens (Nikon Plan Apo, 40×, with a numerical aperture of 0.65) that focuses it onto the intended optical trapping pattern. A beam splitter transmits the laser light to the target's input pupil, while

$$\mathrm{F}\ (x_0, y_0) = \frac{n_m r^2}{2c} \int_0^{\pi/2} \int_0^{2\pi} \left[T^2 \left(\frac{sin2(\theta_o - \theta_i) - Rsin2\theta_i}{1 + R^2 + 2Rcos2\theta_o} \right) Rsin2\theta_i \right] \times I(x,y)\, sin2\theta_i cos\varphi d\varphi d\theta_i \qquad (1)$$

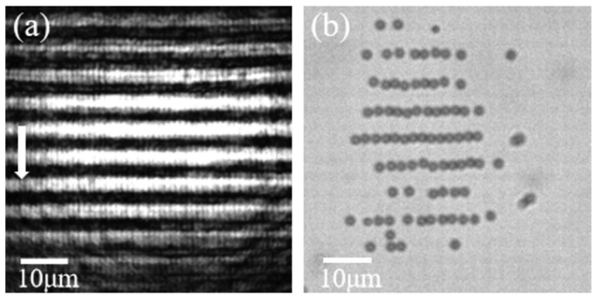

Fig. 3. Optical trapping of polystyrene spheres by using fringe optical field with the size of $\Lambda = 3$ μm. (a) Generation of dynamic fringe optical field with different sizes and velocities by using spatial light modulator. The arrow indicates the movement direction of the fringes. (b) Trapping of polystyrene spheres with 2 μm in diameter. The laser power is 40 mW, and the scale bar is 10 μm.

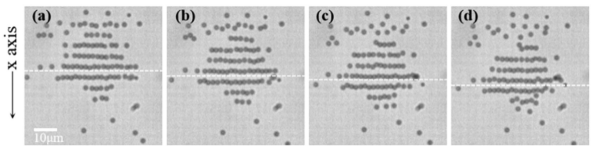

Fig. 4. Transport of polystyrene spheres with 2 μm diameter, using the dynamic fringe optical field with a velocity of v = 1. 5 μm/s and the maximum delivery distance of up to 6.88 μm. (a) t = 0 s, (b) t = 3.6 s; (c) t = 5.6 s; (d) t = 7 s, the white dotted line is used as a reference.

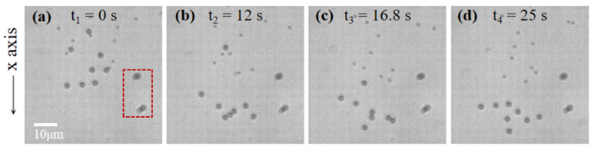

Fig. 5. Sorting of polystyrene spheres with diameters of 0.8 and 2 μm using the dynamic fringes that have a size $\Lambda = 3$ μm and velocity v = 1.5 μm/s. Frames (a)-(d) show sorting of two sizes of particles at different times (a) $t_1 = 0$ s; (b) $t_2 = 12$ s; (c) $t_3 = 16.8$ s and (d) $t_4 = 25$ s. x-axis represents the moving direction of fringes, and the two dots in the red frame are background dust from the CCD.

allowing images at other wavelengths to pass through to a video camera (Norpix FR180, 2048 × 1088, >165 samples/s, pixels with a size of 5.5 × 5.5 μm^2). Thereafter, the fringe optical traps were projected into an aqueous dispersion of colloidal polystyrene spheres sealed into a 300-μm-thick gap between a glass microscope slide and a glass coverslip. To manipulate the polystyrene spheres accurately, the sample cell was placed on a translation stage in the experiment. A white LED (GCI-060411, 440-670 nm, 1 W) was used to illuminate the sample cell. To ensure the quality of the images, a bandpass filter was placed in front of the charge-coupled device (CCD) camera.

IV. Results and Discussion

A. Optical Trapping

To generate a dynamic fringe optical field with tunable sizes and velocities, we use a spatial light modulator (SLM) to shape a Gaussian beam with the polarization parallel to the x-axis. Using a customized MATLAB control program, the periodic fringe phase masks were designed and loaded onto the SLM sequentially. As indicated in Fig. 3(a), the generated dynamic fringe field predicts the same patterns as depicted in Fig. 1(a) by using the theoretical parameters. By focusing on the MO lens, we can obtain a bright fringe trap with a size of 3 μm. The effective region of the optical field is also a Gaussian profile with a beam waist of 40 μm (Fig. 3(a)). In addition, the fringe optical traps can move with a tunable speed along the x-axis, as shown by the white arrow in Fig. 3(a).

To ensure appropriate sorting performance, we begin by observing the trapping of polystyrene particles using this fringe optical field. In our experiments, a sample cell (0.3-mm-thick along the optical axis z) with a rectangular section was filled with an aqueous suspension of polystyrene beads, each 2 μm in diameter. The temperature was maintained at 25°C for all the particle suspensions. To neglect the effect of interactions among individual particles, 1% concentration by weight fraction was ensured. A characteristic optical trapping pattern is presented in Fig. 3(b), representing several chain-like structures in the bright fringe regions with a laser power of 40 mW and a stripe size of 3 μm. Because of the stronger intensity-gradient force, the polystyrene particles are closely arranged in the center of the laser beam. These chain-like structures are stable and will not collapse as long as the existence of the optical sieve. Fig. 4 shows the directional movement of polystyrene particles, which also clearly presents the stability of the trapped particles within 7 s. Since the particles can be stably trapped by fringe optical field, there is almost no displacement in the x-y plane in the center of the optical field. In contrast, in the marginal area, the particles are less ordered, as shown in Fig. 3(b).

B. Particles Directional Movement

Next, we investigated the transport behavior of polystyrene particles based on a dynamic fringe optical field with a laser power of 40 mW. As shown in Fig. 4(a), polystyrene particles with 2 μm diameter were first trapped by bright fringe patterns with a spatial size of 3 μm. The white dotted line represents the initial position of the trapped particles (Fig. 4(a)). We subsequently set the fringes to move along the x-axis at a speed of 1.5 μm/s. Fig. 4(b) shows that the dynamic fringe traps propel the polystyrene particles to leave the initial point and move along the x-axis when the observation time is 3.6 s. When the observation time was further increased to t = 5.6 s, the delivery distance increased (Fig. 4(c)). In the present scheme, the largest delivery distance with 2-μm polystyrene particles reaches 6.88 μm at t = 7 s (Fig. 4(d)) that is much longer than that of a single optical tweezer (1.5–2.4 μm [34]). It should be noted that limited by the range of effective optical field, the transport distance of particles is shorter than the displacement of fringe (i.e., ∼10 μm from 1.5 μm/s × 7 s). In our experiment, the transport distance can be flexibly controlled by changing the power of laser beam and the velocities of fringe. In addition, the polystyrene particles present an ordered arrangement in the region of effective optical field, as observed based on the experimental data (Fig. 4(a)–(d)). Thus, we can use the designed dynamic optical field to assemble and manipulate multiple particles in suspension solutions.

C. Optical Sorting

The sorting capabilities of our method are demonstrated in Fig. 5, where the bright fringe with a velocity of 1.5 μm/s is

used to show the separation of the polystyrene particles with 0.8 and 2 μm diameter. To obtain an appropriate performance, the concentration of the mixture was ensured as 0.1% by weight fraction. As indicated in Fig. 5(a)–(d), the dynamic fringe field behaves similar to an optical sieve that can trap particles with 2 μm diameter and sweep them toward the x-axis, to sort the particles of different sizes in our experiment. The final separation of the particles with diameters of 0.8 and 2 μm was observed at $t_4 = 25$ s (Fig. 5(d)), where the larger particles were localized away from the x-axis. Further, at certain observation time points, the motion of the 2-μm particles is found to result from the movement of the fringe optical traps. Initially (Fig. 5(a)), the two polystyrene particles are mixed together, and the larger particles are trapped by the bright fringes. At certain observation time instants (e.g., t = 12 s, as shown in Fig. 5(b)), the dynamic fringes propel the larger particles (2 μm in diameter), moving them away from the x-axis. In contrast, the small particles with a diameter of 0.8 μm still exhibit Brownian motion in the opposite direction of the moving fringe. To further examine the particle sorting ability, we chose another dynamic fringe optical field with a size of 3.9 μm at a speed of 2 μm/s. The input laser was operated at a power of 40 mW.

V. Conclusion

In summary, we have demonstrated a flexible method for optical trapping and sorting of micro–nano particles in a dynamic fringe optical field that does not involve microfluidic flow. Dynamic modulation of the velocity and size of fringe-like patterns provides an easy approach to control the motion of multiple particles with high flexibility in a mixture suspension. This method could be used to analyze particles of a given size or refractive index by tuning the optimum control parameters, such as velocity or size of the fringes and incident power of the laser. In addition, our sorting strategy can also be used for metal particles, e.g., Ag nanoparticles. Therefore, the dynamic optical sieve presents a flexible approach for optical sorting of multiple particles that provides a promising means for precise micro-nanoparticle sorting and delivery in a biological system and enables simultaneous selection of size-specified nanoparticles for optical manipulation at the multiple-particle level.

References

[1] T. Cizmar, L. C. Romero, K. Dholakia, and D. L. Andrews, "Multiple optical trapping and binding: New routes to self-assemble," *J. Phys. B-At., Mol. Opt. Phys.*, vol. 43, no. 10, Apr. 2010, Art. no. 102001.

[2] R. W. Bowman and M. J. Padgett, "Optical trapping and binding," *Rep. Prog. Phys.*, vol. 76, no. 2, Feb. 2013, Art. no. 026401.

[3] R. X. Zhu, T. Avsievich, A. Popov, and I. Meglinski, "Optical tweezers in studies of red blood cells," *Cell*, vol. 9, no. 3, Mar. 2020, Art. no. 545.

[4] D. R. Gossett, W. M. Weaver, G. Hua, L. Qiyue, and P. Ian, "Label-free cell separation and sorting in microfluidic systems," *Anal. Bioanalytical Chem.*, vol. 3, no. 4, Dec. 2010, Art. no. 041504.

[5] N. Suwanpayak, M. A. Jalil, C. Teeka, J. Ali, and P. P. Yupapin, "Optical vortices generated by a PANDA ring resonator for drug trapping and delivery applications," *Biomed. Opt. Exp.*, vol. 2, no. 1, pp. 159–168, Jan. 2011.

[6] N. T. Nguyen, S. A. M. Shaegh, N. Kashaninejad, and D. T. Phan, "Design, fabrication and characterization of drug delivery systems based on lab-on-a-chip technology," *Adv. Drug Del. Rev.*, vol. 65, no. 11/12, pp. 1403–1419, Nov. 2013.

[7] F. M. Fazal and S. M. Block, "Optical tweezers study life under tension," *Nat. Photon.*, vol. 5, no. 6, pp. 318–321, Jun. 2011.

[8] P. C. Ashok and K. Dholakia, "Optical trapping for analytical biotechnology," *Curr. Opin. Biotechnol.*, vol. 23, no. 1, pp. 16–21, Feb. 2012.

[9] H. M. Nussenzveig, "Cell membrane biophysics with optical tweezers," *Eur. Biophys. J. Biophys. Lett.*, vol. 47, no. 5, pp. 499–514, Jul. 2018.

[10] Y. J. Shen, Z. S. Wan, Y. Meng, X. Fu, and M. L. Gong, "Polygonal vortex beams," *IEEE Photon. J.,* vol. 10, no. 4, Aug. 2018, Art. no. 1503016.

[11] D. G. Grier, "A revolution in optical manipulation," *Nature*, vol. 424, no. 6950, pp. 810–816, Aug. 2003.

[12] S. A. Tatarkova, W. Sibbett, and K. Dholakia, "Brownian particle in an optical potential of the washboard type," *Phys. Rev. Lett.*, vol. 91, no. 3, Jul. 2003, Art. no. 038101.

[13] N. Bhebhe, P. A. C. Williams, C. Rosales-Guzman, V. Rodriguez-Fajardo, and A. Forbes, "A vector holographic optical trap," *Sci. Rep.*, vol. 8, Nov. 2018, Art. no. 17387.

[14] D. Patra, S. Sengupta, W. T. Duan, H. Zhang, R. Pavlick, and A. Sen, "Intelligent, self-powered, drug delivery systems," *Nanoscale*, vol. 5, no. 4, pp. 1273–1283, Oct. 2013.

[15] K. Kim, J. H. Guo, Z. X. Liang, and D. L. Fan, "Artificial micro/nanomachines for bioapplications: Biochemical delivery and diagnostic sensing," *Adv. Funct. Mater.*, vol. 28, no. 25, pp. 1–19, Jun. 2018.

[16] J. H. Kim *et al.*, "Remote manipulation of droplets on a flexible magnetically responsive film," *Sci. Rep.*, vol. 5, Dec. 2015, Art. no. 17843.

[17] S. Ben *et al.*, "Cilia-inspired flexible arrays for intelligent transport of viscoelastic microspheres," *Adv. Funct. Mater.*, vol. 28, no. 16, Apr. 2018, Art. no. 1706666.

[18] S. Z. Zhang, Y. Wang, P. R. Onck, and J. M. J. den Toonder, "Removal of microparticles by ciliated surfaces—An experimental study," *Adv. Funct. Mater.*, vol. 29, no. 6, Feb. 2019, Art. no. 1806434.

[19] A. Ashkin, "Acceleration and trapping of particles by radiation pressure," *Phys. Rev. Lett.*, vol. 24, no. 4, pp. 156–159, Jan. 1970.

[20] E. R. Dufresne and D. G. Grier, "Optical tweezer arrays and optical substrates created with diffractive optics," *Rev. Sci. Instrum.*, vol. 69, no. 5, pp. 1974–1977, May 1998.

[21] S. B. Cheng, S. H. Tao, X. Y. Zhang, and W. Z. Ma, "Optical tweezers with fractional fractal zone plate," *IEEE Photon. J.*, vol. 8, no. 5, Oct. 2016, Art. no. 6100407.

[22] P. Zemanek, V. Karasek, and A. Sasso, "Optical forces acting on rayleigh particle placed into interference field," *Opt. Commun.*, vol. 240, no. 4-6, pp. 401–415, Oct. 2004.

[23] E. Madadi, M. Biagooi, F. Mohammadjafari, and S. N. Oskoee, "Particle size effect on sorting with optical lattice," *Sci. Rep.*, vol. 10, no. 1, Oct. 2020, Art. no. 18294.

[24] A. N. Rubinov, "Physical grounds for biological effect of laser radiation," *J. Phys. D-Appl. Phys.*, vol. 36, no. 19, pp. 2317–2330, Oct. 2003.

[25] H. Kim, W. Lee, H. G. Lee, H. Jo, Y. Song, and J. Ahn, "In situ single-atom array synthesis using dynamic holographic optical tweezers," *Nat. Commun.*, vol. 7, Oct. 2016, Art. no. 13317.

[26] J. A. Rodrigo, M. Angulo, and T. Alieva, "Dynamic morphing of 3D curved laser traps for all-optical manipulation of particles," *Opt. Exp.*, vol. 26, no. 14, pp. 18608–18620, Jul. 2018.

[27] A. Casaburi, G. Pesce, P. Zemanek, and A. Sasso, "Two-and three-beam interferometric optical tweezers," *Opt. Commun.*, vol. 251, no. 4-6, pp. 393–404, Jul. 2005.

[28] J. Peter, C. Tomas, S. Mojmir, and Z. Pavel, "Static optical sorting in a laser interference field," *Appl. Phys. Lett.*, vol. 92, no. 16, Apr. 2008, Art. no. 161110.

[29] P. Jakl, A. V. Arzola, M. Siler, L. Chvatal, K. Volke-Sepulveda, and P. Zemanek, "Optical sorting of nonspherical and living microobjects in moving interference structures," *Opt. Exp.*, vol. 22, no. 24, pp. 29746–29760, Dec. 2014.

[30] K. Volke-Sepulveda, S. Chavez-Cerda, V. Garces-Chavez, and K. Dholakia, "Three-dimensional optical forces and transfer of orbital angular momentum from multiringed light beams to spherical microparticles," *J. Opt. Soc. Amer. B-Opt. Phys.*, vol. 21, no. 10, pp. 1749–1757, Oct. 2004.

[31] R. Gussgard, T. Lindmo, and I. Brevik, "Calculation of the trapping force in a strongly focused laser beam," *J. Opt. Soc. Amer. B-Opt. Phys.*, vol. 9, no. 10, pp. 1922–1930, Oct. 1991.

[32] I. Ricardez-Vargas, P. Rodriguez-Montero, and R. Ramos-Garcia, "Modulated optical sieve for sorting of polydisperse microparticles," *Appl. Phys. Lett.*, vol. 88, no. 12, Mar. 2006, Art. no. 121116.

[33] X. L. Chen *et al.*, "Coaxial differential dynamic microscopy for measurement of brownian motion in weak optical field," *Opt. Exp.*, vol. 26, no. 24, pp. 32083–32090, Nov. 2018.

[34] Ø. I. Helle, B. S. Ahluwalia, and O. G. Hellesø, "Optical transport, lifting and trapping of micro-particles by planar waveguides," *Opt. Exp.*, vol. 23, no. 5, pp. 6601–6612, Mar. 2015.